Low-complexity Behavioral Model for Predictive Maintenance of Railway Turnouts

Pegah Barkhordari[1], Roberto Galeazzi[1], Alejandro de Miguel Tejada[2], and Ilmar F. Santos[2]

[1] *Dept. Electrical Engineering, Technical Univerisity of Denmark, Kgs. Lyngby, Denmark*
pebark@elektro.dtu.dk
rg@elektro.dtu.dk

[2] *Dept. Mechanical Engineering, Technical Univerisity of Denmark, Kgs. Lyngby, Denmark*
almite@mek.dtu.dk
ifs@mek.dtu.dk

ABSTRACT

Maintenance of railway infrastructures represents a major cost driver for any infrastructure manager since reliability and dependability must be guaranteed at all times. Implementation of predictive maintenance policies relies on the availability of condition monitoring systems able to assess the infrastructure health state. The core of any condition monitoring system is the a-priori knowledge about the process to be monitored, in the form of either mathematical models of different complexity or signal features characterizing the healthy/faulty behavior. This study investigates the identification of a low-complexity behavioral model of a railway turnout capable of capturing the dominant dynamics due to the ballast and railpad components. Measured rail accelerations, acquired through a receptance test carried out on the switch panel of a turnout of the Danish railway network, have been utilized together with the Eigensystem Realization Algorithm – a type of subspace identification – to identify a fourth order model of the infrastructure. The robustness and predictive capability of the low-complexity behavioral model to reproduce track responses under different types of train excitations have been successfully validated. It is anticipated that the identified model will be instrumental for the development of methods for diagnosis and prognosis of faults and degradation process in switches and crossings.

1. INTRODUCTION

Railway networks heavily rely on the dependability of infrastructure components to safely control the train traffic and optimize the network capacity. Therefore the reliability of track components must be guaranteed at all times. This clearly makes railway infrastructure components a major cost driver of maintenance and renewal actions for all railway infrastructure managers (EIM-EFRTC-CER Working Group, 2012). Figure 1 shows the maintenance cost in European countries with track utilization (total train kilometers divided by track kilometers) similar to Denmark. The reported data were selected from (Juul Andersen, 2012; EIM-EFRTC-CER Working Group, 2012) following the clustering proposed in (Steer Davies Gleave, 2015), where countries are grouped according to socioeconomic and railway infrastructure parameters. A large amount of this expenditure is assigned to maintenance and renewal actions of switches and crossings (S&Cs). Banedanmark, the Danish railway infrastructure manager, estimates that each year one third of the total track maintenance cost is spent on turnouts. S&Cs are complex elements whose failure weighs heavily on transport safety, as reported in the RSSB Annual Safety Performance Report (Clinton, 2014, Section 8.5) where 31% of the track-related derail-

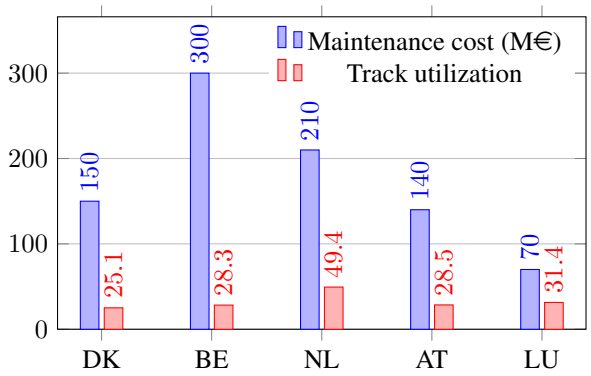

Figure 1. Railway maintenance cost for European countries with track utilization similar to Denmark. Track utilization is defined as the ratio between the total train kilometers and the track kilometers (data refers to year 2012).

ments are due to S&Cs malfunctioning in the period 2009–2014 in Great Britain. Failure data recorded in the UK in 2009 (Hassankiadeh, 2011, Chapter 7) showed that ballast degradation is the third most important component affecting the turnouts performance with a failing frequency of 7.9%[1].

As railway is expected to play a key role for the future development of sustainable transport in Europe, it is essential to keep improving safety while reducing cost. There is a growing interest in changing maintenance policies from reactive or periodic to predictive; this occurs in connection with the widespread digitalization of the infrastructure that gives the operators access to information and field data previously unavailable. Predictive maintenance relies on methods and algorithms that, based on measured data and a-priori knowledge, can forecast with low uncertainty the remaining useful lifetime of components and systems. Condition monitoring (CM) systems, capable to provide early warnings of the development of deterioration processes and the inception of faults, become then a valuable asset to reduce maintenance cost and ensure the efficient utilization of the railway infrastructure.

1.1. State of the art

Operational experience and research studies point out that a key element affecting the infrastructure performance is the track stiffness, which to greater extent is attributed to the ballast and subballast layers. Monitoring of these track components is challenging since degradation processes affecting their elastic behavior are hard to assess through non destructive measurement methods. In literature several approaches to monitoring of track stiffness for the open track were proposed; these methods are categorized as *direct* and *indirect*.

Direct approaches include the scanning of the subsurface through the ground penetrating radar (GPR) (Smekal, Berggren, & Silvast, 2006; Berggren, 2009; Kind, 2011); the assessment of the bearing capacity of the soil through the cone penetration test[2] (CPT) (Brough, Stirling, Ghataora, & Madelin, 2003); the visual inspection of track condition at surface level (Labarile, Stella, Ancona, & Distante, 2004; Yella, Dougherty, & Gupta, 2009; Asplund, Larsson, Rantatalo, Nissen, & Kumar, 2013). Although these techniques may support infrastructure managers to schedule and perform maintenance tasks, they have some significant limitations. The GPR method presents difficulties in properly locating the ballast damage due to challenges in selecting a suitable frequency range for the electromagnetic waves. The CPT method is a destructive and time consuming test that affects train operations. Last, the visual inspection is only effective in detecting damage when it has already surfaced. Indirect techniques rely on the "smart processing" of measured quantities gathered on the railway superstructure (track and sleepers) by non destructive methods. Hosseingholian et al. (2009) proposed the use of a vibrating rolling wheel to excite the track and compute its stiffness based on measured wheel accelerations. Berggren et al. (2014) used two independent measurements of longitudinal track level acquired through a track recording car to estimate and monitor track displacement and stiffness due to train loading.

Recently, model-based approaches to ballast damage detection have been proposed by Lam et al. (2012, 2014), where the rail-sleeper-ballast system was modeled as Timoshenko beam on an elastic foundation and changes in the ballast stiffness were monitored through a model update procedure. In (Lam et al., 2012) a feasibility study was performed using both simulated and experimental data; whereas the estimate of the ballast stiffness was robustified in (Lam et al., 2014) by casting the model update in the Bayesian framework to account for model uncertainty. The author also proposed Bayesian approach based on Monte Carlo method to identify the stiffness of the railway ballast. The results were validated utilizing the measured acceleration in a field test (Lam, Alabi, & Yang, 2017). Although some attempts have been made for condition monitoring of ballast stiffness using model-based techniques, the proposed mechanical models have a large dimensionality resulting in a high complexity of the diagnostic method. Low-complexity data-based behavioral models may be preferred to high-fidelity mechanical models since they enable portability of results across the entire railway network despite natural presence of uncertainties due to e.g. geographical location and physical age of the components.

1.2. Main contribution

This work focuses on the generation of a low-complexity behavioral model of the track dominant dynamics by means of subspace identification techniques. Full-scale acceleration data, collected during a receptance test carried out on the switch panel of a turnout of the Danish railway network, are utilized for model identification. The obtained model properly captures the dynamic behavior of the infrastructure in the frequency range $[0, 1000]$ Hz. In particular, the resonant peaks corresponding to the ballast layer and the railpad are correctly identified providing the model with good predictive capabilities. These are tested by validating the model on full-scale acceleration data recorded during a train passage.

All measured data presented in the paper are anonymized to comply with the policy of the Danish railway infrastructure manager.

[1] The first two components affecting turnout performance are the switch rail (45.3%) and the slide chair (30.4%).

[2] In geotechnical engineering the bearing capacity of the soil is the ability of the soil to withstand loads applied to the ground. The cone penetration test uses mechanical measurements of total penetration resistance to pushing a tool with a conical tip into soil.

2. EXPERIMENTAL CAMPAIGN

In this section, the receptance test campaign performed at one of the switches and crossings belonging to the Danish railway network is described. The receptance test is commonly used for railway tracks to characterize the main dynamic properties of the different track components. Through this, it is possible to determine the health state of a particular railway turnout by means of the assessment of its dynamic response to impact excitation. Data coming from the aforementioned test is used in this study to identify a low-complexity behavioral model, which is anticipated to be a key element for the development of a condition monitoring system for the predictive maintenance of S&Cs.

The receptance test consists in the excitation of the railway track by impacting the top of the rail with an instrumented impact hammer and the measurement of the response by using accelerometers, typically placed on the rail head. Measured forces and accelerations are then combined and analyzed, in the frequency domain, to identify the main resonant and antiresonant frequencies of the track. The informative level of the measured acceleration is assessed by means of the coherence function, which allows to determine the frequency ranges where the receptance data are significant.

The analysis of the receptance function – also known as dynamic flexibility or mobility (Ewins, 2000) – is a non-destructive methodology that gives insight into the dynamic properties of the track by pinpointing the main resonant frequencies (De Man, 2002; Kaewunruen & Remennikov, 2007). Furthermore, the data gathered during the experimental receptance campaigns can be used to calibrate sophisticated numerical models of the track by setting up the stiffness and damping values of the different components that are part of the track (Alves Costa, Calçada, & Silva Cardoso, 2012; Verbraken, Degrande, Lombaert, Stallaert, & Cuellar, 2013). Results from receptance test can be also used to detect defects on the rail surface (Oregui, Li, & Dollevoet, 2015) or to analyze the effect of substructure changes in the lower frequency content of the receptance curve (Arlaud, Costa D'Aguiar, & Balmes, 2016).

2.1. Receptance test at Tommerup station's turnout

The receptance test was carried out using a large sledge impulse hammer (Model nr: 086D50 PCB Piezometrics, range: ±22.240 N, sensitivity: 0.2083 mV/N, mass: 5.5 kg, hard tip). The location of the impact along the switch and crossing is coincident with point A1, just before the switch panel, as illustrated in Fig. 2. The rail was impacted right above the sleeper such that the main vibration modes of the track could be properly excited. To verify the measured acceleration two different accelerometers were utilized for the receptance test, both located near the impact point. The first is a 2-axis accelerometer (KISTLER 8702B500, range:±500 g,

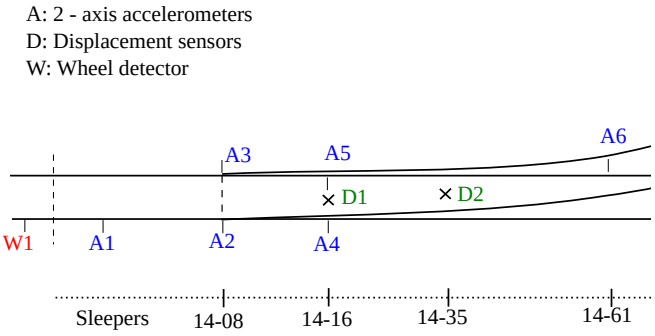

Figure 2. Layout of the sensors location along the turnout at Tommerup station. The data utilized in this work refer to accelerations measured by accelerometers A1 and A4 on the straight track.

(a) Overview of the turnout in proximity of Tommerup station

(b) Setup for the receptance test including hammer and accelerometers

Figure 3. Pictures from the receptance test carried out in February 2017 nearby Tommerup station (Fyn - Denmark).

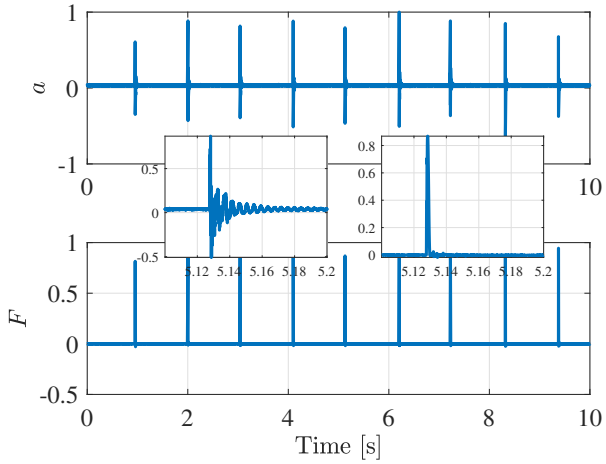

Figure 4. Outcome of the receptance test: (top) measured acceleration on the rail head; (bottom) measured impact force.

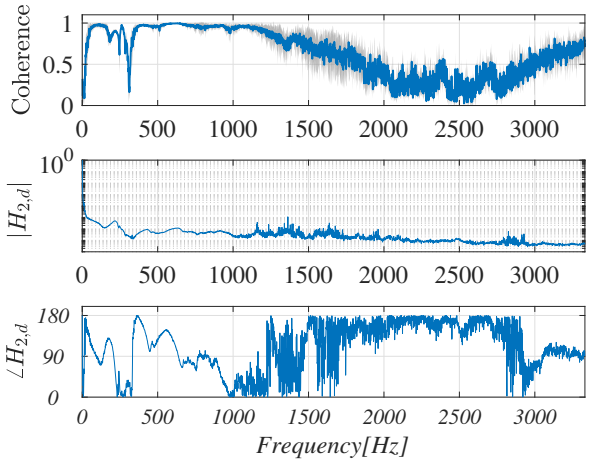

Figure 5. Analysis of receptance data: (top) input-output coherence, (mid) magnitude of $H_{2,d}$, (bottom) phase of $H_{2,d}$.

sensitivity:10 $\pm$0.05 mV/g , weight: 8.2 grams) magnetically attached to the rail web; whereas the second is a single axis accelerometer (Type: 4339 Brül & Kjær, range: $\pm$50 g, sensitivity: 10.02 mV/g, weight: 12.7 grams) located on the top of the rail and used for verification purposes (see Fig. 3b). A set of measurements was carried out considering a minimum of 5 impacts. The sampling frequency used to log both force and acceleration was set to 20 kHz. An example of input-output data gathered during a single receptance test is shown in Fig. 4, where the acceleration is measured atop the rail.

Combining the input force F and the output acceleration a it is possible to determine the coherence function, which evaluates in the frequency domain how well the measured acceleration corresponds to the applied force. The coherence function is given by

$$C_{Fa}(\omega) = \frac{|\, G_{Fa}(\omega)^2 \,|}{G_{FF}(\omega) G_{aa}(\omega)} \tag{1}$$

where $G_{aa}(\omega)$ is the auto power spectrum of the acceleration, $G_{FF}(\omega)$ is the auto power spectrum of the force and G_{Fa} (ω) is the cross power spectrum between the force and the acceleration (Ewins, 2000). The coherence function always satisfies the constraint $0 \leq C_{Fa}(\omega) \leq 1$. It is common practice to threshold the coherence function to determine the frequency ranges where the input-output relation is "well defined"; however the threshold value is application dependent. According to Oostermeijer and Kok (2000) coherence between 0.85 and 1 indicates that results coming from a hammer test are reliable; whereas Arlaud et al. (2016) rejected results when the coherence dropped below 0.9. A threshold of 0.9 is here chosen to indicate a low quality of the results due to external nuisance factors that may have affected the measurement campaign.

To reduce the influence of uncontrollable nuisance factors possibly affecting the outcome of the experimental data, as e.g. the natural differences in the magnitude and width of the impacts[3], the coherence function $C_{Fa}(\omega)$ is computed by averaging the coherence functions associated with each impact response, i.e.

$$C_{Fa}^{\text{avg}}(\omega) = \frac{1}{M} \sum_{i=1}^{M} C_{Fa,i}(\omega) \tag{2}$$

where $C_{Fa,i}$ is the coherence function of the i-th input-output pair (F_i, a_i) and M is the total number of impacts.

Figure 5 shows the coherence function with the 95% confidence interval. From its analysis it can be concluded that across all experiments there is a clear input-output relation up to 1 kHz. Therefore, the following model identification procedure should consider information content of the measured acceleration only within the frequency range $[0, 1000]$ Hz.

By means of $G_{aa}(\omega)$ and $G_{Fa}(\omega)$ an estimator of the frequency response function is computed

$$H_{2,a}(\omega) = \frac{G_{aa}(\omega)}{G_{Fa}(\omega)}, \tag{3}$$

which, in turn, is used to obtain the displacement frequency response function

$$H_{2,d}(\omega) = \frac{H_{2,a}(\omega)}{-\omega^2}. \tag{4}$$

$H_{2,d}(\omega)$ is a good indicator for detecting presence of resonant frequencies (Ewins, 2000). By analyzing its magnitude and phase in the frequency range $[0, 1000]$ Hz (Fig. 5) two significant peaks are distinguished. The first peak detected

[3]The impact hammer is manually operated as shown in Fig. 3b; hence despite all efforts it is not possible to ensure the exact repeatability of the test.

around $200\,\mathrm{Hz}$ may be linked to the full track resonant mode shape. Dahlberg (2006) locates this frequency in the range of $[50, 300]\,\mathrm{Hz}$, whereas Choi (2014) detects this resonant frequency within the interval $[40, 400]\,\mathrm{Hz}$. The second resonant frequency of interest can be detected around 600 Hz and it may correspond to the mode shape in which the rail bounces on the railpads. This matches the results by Dahlberg (2006) that locate this frequency in the range $[200, 600]\,\mathrm{Hz}$ and (Choi, 2014), where it is stated that in frequency intervals above $400\,\mathrm{Hz}$ the railpad behavior is dominant.

Notwithstanding, a third peak located between the two aforementioned resonant frequencies can be observed in Fig. 5 (mid plot), around $400\,\mathrm{Hz}$. In the literature there are indications that this frequency may correspond to an additional vibration mode caused by intermediate elements located between the ballast layer and the railpad, as it is the case of the elastic baseplate. This element, belonging to the fastening system, is not within the scope of the present work and therefore its characteristic frequency is conveniently omitted in the following sections. Summarizing, from the frequency analysis of the receptance test results it can be concluded that: $[0, 1000]\,\mathrm{Hz}$ is the frequency range where measured accelerations data can be utilized reliably; there are two resonant frequencies associated to the ballast layer and the railpads around 200 Hz and 600 Hz, respectively.

3. SUBSPACE IDENTIFICATION

The track vertical acceleration measured during the receptance test is the free impulse response of the track and as such it contains information about the natural eigenmodes of the system. Receptance tests are seldom performed by infrastructure managers due to cost and potential disruption of service; hence S&Cs' motion data are generally available in connection with train passages. However, in this case no information about the exciting force is accessible since the load exerted by the train wheel sets is unknown. This suggests that the measured acceleration should be rather considered as the zero-input output response of the track, where the initial condition coincides with the magnitude of the response induced at the time of impact.

Consider the linear time-invariant discrete time system

$$\mathbf{x}_{i+1} = \mathbf{A}\mathbf{x}_i + \mathbf{b}u_i \tag{5}$$

$$y_i = \mathbf{c}\mathbf{x}_i \tag{6}$$

where $\mathbf{x}_i \in \mathbb{R}^n$, $u_i \in \mathbb{R}$ and $y_i \in \mathbb{R}$ are the state vector, the input and output at time $i \in \mathbb{N}$. The matrices $\mathbf{A}$, $\mathbf{b}$ and $\mathbf{c}$ are of opportune dimensions related to the former vectors. Said $\mathbf{x}_0$ the system's initial condition, the zero-input output response and the free pulse response are given by

$$y_i = \mathbf{c}\mathbf{A}^i\mathbf{x}_0 \tag{7}$$

$$y_i = \mathbf{c}\mathbf{A}^{i-1}\mathbf{b} \tag{8}$$

i.e. at each time step the system output is given by a linear combination of the system eigenmodes. This implies that by exploiting the measured outputs it is possible to reconstruct a minimal realization of the system $(\hat{\mathbf{A}}, \hat{\mathbf{b}}, \hat{\mathbf{c}})$ that is equivalent to the true realization $(\mathbf{A}, \mathbf{b}, \mathbf{c})$ through a similarity transformation.

In this work the Eigensystem Realization Algorithm (ERA) proposed by Juang and Pappa (1985) is adopted to identify a low-complexity behavioral model of the track based on measured vertical accelerations. The ERA is a system identification technique that is largely adopted in civil engineering, in particular for structural health monitoring purposes. The method was applied for the system identification of e.g. aerospace structures (Pappa & Juang, 1984) and civil structures (Caicedo, Dyke, & Johnson, 2004).

In structural engineering ERA is used to identify natural frequencies, mode shapes and damping ratios. The ERA is commonly used in conjunction with the natural excitation technique to identify modal parameters from ambient vibration. The technique has been applied to buildings, bridges, and other types of structural systems. In the area of structural health monitoring ERA and other modal identification techniques play an important role in developing a model for structures from experimental data. The state space representation or the modal parameters are used for further analysis and to identify possible deterioration in structures.

3.1. Overview of ERA method

The following review of the Eigensystem Realization Algorithm is based on the original formulation by Juang and Pappa (1985). It is worth noting that the identification methodology does not change if the zero-input output response is used instead of the free pulse response, since in the former case the $\mathbf{b}$ vector represent the information of the initial condition $\mathbf{x}_0$ (compare Eq. (7) with Eq. (8)).

Given the free pulse response in Eq. (8) the Hankel matrix $\mathbf{H}_0$ and the shifted Hankel matrix $\mathbf{H}_1$ of the Markov parameters are constructed as follows (Juang & Pappa, 1985)

$$\mathbf{H}_0 = \begin{bmatrix} y_1 & y_2 & \cdots & y_n \\ y_2 & y_3 & \cdots & y_{n+1} \\ \vdots & \vdots & \ddots & \vdots \\ y_n & y_{n+1} & \cdots & y_{2n-1} \end{bmatrix}$$

$$= \begin{bmatrix} \mathbf{cb} & \mathbf{cAb} & \dots & \mathbf{cA}^{n-1}\mathbf{b} \\ \mathbf{cAb} & \mathbf{cA}^{2}\mathbf{b} & \dots & \mathbf{cA}^{n}\mathbf{b} \\ \vdots & \vdots & \ddots & \vdots \\ \mathbf{cA}^{n-1}\mathbf{b} & \mathbf{cA}^{n}\mathbf{b} & \dots & \mathbf{cA}^{2n-2}\mathbf{b} \end{bmatrix} \quad (9)$$

$$\mathbf{H}_1 = \begin{bmatrix} y_2 & y_3 & \cdots & y_{n+1} \\ y_3 & y_4 & \cdots & y_{n+2} \\ \vdots & \vdots & \ddots & \vdots \\ y_{n+1} & y_{n+2} & \cdots & y_{2n} \end{bmatrix} \quad (10)$$

where the dimension of the Hankel matrices is $n \times n$. The matrix $\mathbf{H}_0$ can be rewritten as

$$\mathbf{H}_0 = \begin{bmatrix} \mathbf{c} \\ \mathbf{cA} \\ \vdots \\ \mathbf{cA}^{n-1} \end{bmatrix} \begin{bmatrix} \mathbf{b} & \mathbf{Ab} & \dots & \mathbf{A}^{n-1}\mathbf{b} \end{bmatrix} = \mathbf{\Phi}_o \mathbf{\Phi}_c, \quad (11)$$

where $\mathbf{\Phi}_o$ and $\mathbf{\Phi}_c$ are the observability and controllability matrices, which can be obtained through the Singular Value Decomposition (SVD) of $\mathbf{H}_0$

$$\mathbf{H}_0 = \mathbf{U}\mathbf{\Sigma}^2\mathbf{V}^T = (\mathbf{U}\mathbf{\Sigma})(\mathbf{\Sigma}\mathbf{V}^T) = \mathbf{P}\mathbf{Q}. \quad (12)$$

Noteworthy that this decomposition is not unique.

Using Eq. (11) into Eq. (10) the shifted Hankel matrix is rewritten as

$$\mathbf{H}_1 = \mathbf{\Phi}_o \mathbf{A} \mathbf{\Phi}_c \quad (13)$$

from which the system matrix $\mathbf{A}$ can be computed

$$\mathbf{A} = \mathbf{\Phi}_o^{-1} \mathbf{H}_1 \mathbf{\Phi}_c^{-1}. \quad (14)$$

The inverse of the controllability and observability matrices is guaranteed to exist because they are square matrices by construction and full rank due to the minimality of the realization of the system.

Since $\mathbf{P}$ and $\mathbf{Q}$ ar equivalent to $\mathbf{\Phi}_o$ and $\mathbf{\Phi}_c$ by a similarity transformation then an estimate of the system matrix $\mathbf{A}$ is obtained as

$$\hat{\mathbf{A}} = \mathbf{P}^{-1} \mathbf{H}_1 \mathbf{Q}^{-1}. \quad (15)$$

Estimates of the input and output vectors $\mathbf{b}$ and $\mathbf{c}$ are then obtained by taking the first column of the matrix $\mathbf{Q}$ and the first row of the matrix $\mathbf{P}$.

Given the identified system realization $(\hat{\mathbf{A}}, \hat{\mathbf{b}}, \hat{\mathbf{c}})$ the modal properties of the system in terms of natural frequencies and damping ratios can be computed by

$$w_{nk} = \frac{|\ \ln(\lambda_k(\hat{\mathbf{A}}))\ |}{2\pi T_s} \quad (16)$$

$$\zeta_k = \frac{-\mathrm{Re}(\ln(\lambda_k(\hat{\mathbf{A}}))/T_s)}{|\ \ln(\lambda_k(\hat{\mathbf{A}}))\ |} \quad (17)$$

where T_s is the sampling time and $\lambda_k(\hat{\mathbf{A}})$ is k-th eigenvalue of the matrix $\hat{\mathbf{A}}$. Further, by using the identified model the system output is estimated as (Majji, Juang, & Junkins, 2010)

$$\mathbf{Y} = \mathbf{P}\hat{\mathbf{x}}. \quad (18)$$

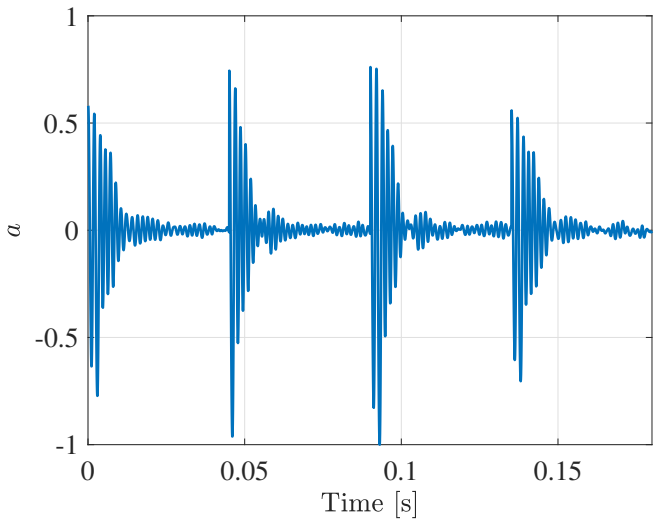

Figure 6. The selected identification data set.

4. LOW-COMPLEXITY BEHAVIORAL MODEL

By applying the ERA identification method to the measured track vertical acceleration data gathered during the receptance test a low-complexity behavioral model of the turnouts dominant dynamics is now developed. The analysis of the coherence function $C_{Fa}^{\mathrm{avg}}(\omega)$ addressed $[0\,,\,1000]$ Hz as the frequency range where the acceleration is clearly related to the impact force; hence the measured acceleration is pre-filtered using a low-pass filter with cut-off frequency of 2 kHz.

Track responses to a single hammer excitation chosen from all the receptance tests are merged and considered as an identification data set (see Fig. 6).

Figure 7 shows the estimated auto power spectrum G_{aa} of the vertical acceleration and its 95% confidence interval. To account for possible variations across the different tests, G_{aa} is computed as the average over all the auto power spectra associated with each hammer impact. The 95% confidence interval is obtained using a chi-squared approach. When the spectrum is plotted on a logarithmic scale, the $(1-\alpha)\times 100$ percent confidence interval is constant at every frequency and it is given by (Manolakis, Ingle, & Kogon, 2005, Chapter 5)

$$\left(10\ln(G_{aa}(e^{j\omega})) - 10\ln\frac{\chi^2_\nu(1-\alpha/2)}{\nu},\right.$$
$$\left. 10\ln(G_{aa}(e^{j\omega})) + 10\ln\frac{\nu}{\chi^2_\nu(\alpha/2)}\right)$$

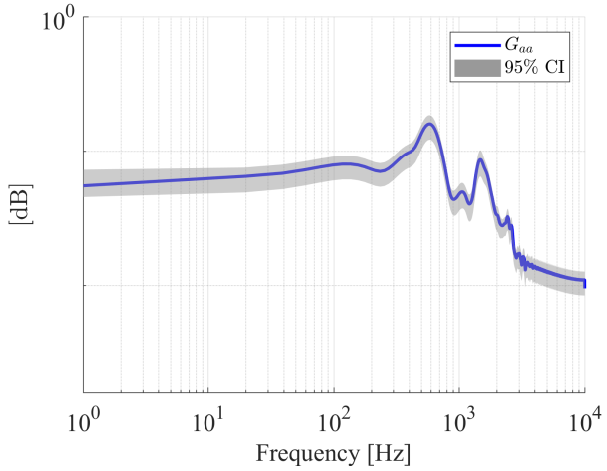

Figure 7. Estimate of the acceleration power spectrum based on the average of all measured responses.

where G_{aa} is the estimate of the auto power spectrum and

$$\nu = \frac{2N}{\sum_{l=-(L-1)}^{L} \omega_a^2(l)}$$

is the degree of freedom of a χ^2_ν distribution. N , L and ω_a are the number of observations, window size and correlation window, respectively.

The auto power spectrum G_{aa} has three significant peaks. Among these, two are located around frequencies lower than 1000 Hz, where the coherence function C_{Fa} confirmed the validity of the receptance test. Consequently, the low-complexity behavioral model should be of fourth order in agreement with the two resonance peaks. In other words, the power spectrum analysis shows that the model to be identified should have one resonance frequency below 200 Hz and another resonance frequency between 200 Hz and 1000 Hz.

As can be seen in Fig. 7, the amplitude of the second resonance peak is significantly larger than the amplitude of the first. Due to this disparity in power levels, to prevent the possible erroneous estimate of the dynamics associate with the low frequency peak, the identification data set is divided in two employing a low-pass and high-pass filter with the cut-off and cut-in frequencies of 200 Hz. Consequently, low (10 - 200 Hz) and high (200 - 1000 Hz) frequency models are identified and their parameters are

$$\mathcal{M}_l : \begin{cases} \hat{\mathbf{A}}_l = \begin{bmatrix} 0.9701 \pm 0.0018 & -0.05308 \pm 0.0007 \\ 0.05308 \pm 0.0007 & 1.0031 \pm 0.009 \end{bmatrix} \\ \hat{\mathbf{C}}_l = \begin{bmatrix} -0.7995 \pm 0.0062 & -0.0208 \pm 0.0002 \end{bmatrix} \end{cases} \tag{19}$$

$$\mathcal{M}_h : \begin{cases} \hat{\mathbf{A}}_h = \begin{bmatrix} 0.9342 \pm 0.0298 & 0.1759 \pm 0.0049 \\ -0.1759 \pm 0.0049 & 1.0210 \pm 0.025 \end{bmatrix} \\ \hat{\mathbf{C}}_h = \begin{bmatrix} -1.9931 \pm 0.007 & -0.1689 \pm 0.005 \end{bmatrix} \end{cases} \tag{20}$$

The two models are then combined in order to provide the final identified model describing the dominant behavior of the vertical track dynamics

$$\mathcal{M} : \begin{cases} \hat{\mathbf{A}} = \begin{bmatrix} \hat{\mathbf{A}}_l & \mathbf{0} \\ \mathbf{0} & \hat{\mathbf{A}}_h \end{bmatrix} \\ \hat{\mathbf{C}} = \begin{bmatrix} \hat{\mathbf{C}}_l & \hat{\mathbf{C}}_h \end{bmatrix} \end{cases} . \tag{21}$$

Using Eq. (16) and considering the model uncertainty the resonance frequencies of the identified model are estimated to be 167.59 ± 9.11 Hz and 549.96 ± 23.20 Hz. Table 1 reports the identified model characteristics: ζ and ω_n are the damping factor and natural frequency associated with the identified eigenmodes.

Table 1. Identified models characteristics.

Model	$\lambda\,[-]$	ω_n [Hz]	$\zeta\,[-]$
$\mathcal{M}_l$	$0.988 \pm 0.0509i$	167.59	0.201
$\mathcal{M}_h$	$0.978 \pm 0.1704i$	549.96	0.044

5. MODEL VALIDATION

The predictive capability and the robustness of the identified model is validated on additional data collected during the receptance test as well as on measured accelerations logged during train passages. The model performance is evaluated through the fitting score in percentage calculated as

$$\text{fit} = 100 \times \frac{1 - \mid a - \hat{a} \mid}{\mid a - \bar{a} \mid} \tag{22}$$

where a is the measured acceleration, $\hat{a}$ is the estimated acceleration and $\bar{a}$ is the mean value of the measured acceleration.

Figure 8 illustrates the model validation against additional receptance test measurements both in the time and frequency domains. Each impact in the validation data set is treated individually as zero-input output response; therefore the initial condition $\mathbf{x}_{0,j}$ is also estimated, where j is the impact index. The auto power spectrum $\hat{G}_{aa}$ of the model output is computed as an average of the power spectra associated with each estimated impact response.

It is evident that the identified low-complexity behavioral model well predicts the behavior of the measured acceleration in correspondence of the two resonant peaks. The pre-

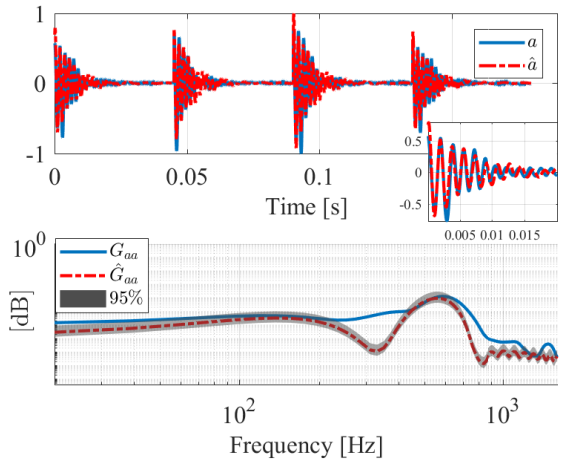

Figure 8. Validation data compared with the identified model and the corresponding frequency responses with 95% of confidence interval.

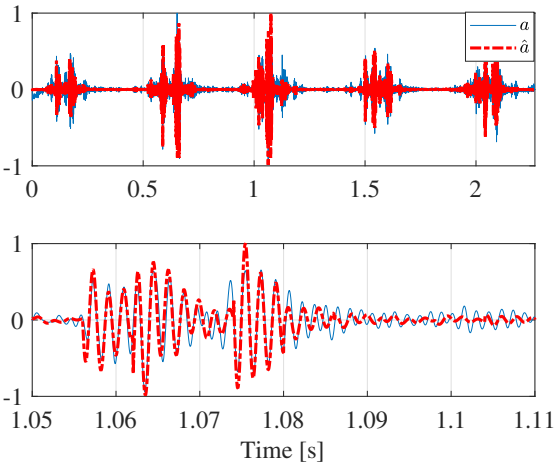

Figure 9. Comparison of the measured and identified accelerations; IC4 train, 110 km/h (a) The whole train passage, (b) Zoom in on a two-wheel set passage.

dicted output $\hat{a}$ fits the validation data set with a fitting score of 75%.

To assess the robustness of the model, its predicting capability is tested on measured vertical accelerations in response to a train excitation recorded at the turnout position A4 (see Fig. 2). Data recorded during 10 train passages differing for train type, traveling speed and loading condition have been considered, and the fitting scores achieved in each case are listed in Table 2. The comparison between predicted output and measured acceleration for an additional data set is shown in Fig. 9 and the fitting score is 67%.

Table 2. Validation result for 10 train passages.

Train type	Speed interval [km/h]	Fitting score [%]
IR4	[110, 120]	56.48
IC4	[140, 150]	70.45
IC3	[110, 120]	59.87
IR4	[50, 60]	65.42
IC4	[50, 60]	63.58
IC3	[50, 60]	52.35
IR4	[150, 160]	51.50
IC4	[150, 160]	72.53
IC3	[150, 160]	55.68
IC3-IC2	[150, 160]	61.24

Based on the obtained results it is concluded that the identified low-complexity behavioral model can appropriately predict the dominant behavior of the track response around the matched resonance frequencies and it is robust to different types of excitations.

5.1. Discussion

To analyze the dynamic interaction between the train and track, two different types of modeling approaches are commonly used. The first is the finite element method (FEM), which is suitable when an in-depth theoretical knowledge of the track components is required. Conversely, if a better understanding of the train-track interfaces is desired then multibody simulation softwares (MBS) represent a more convenient solution due to their lower computational time. MBS thus represents a suitable methodology to assess dynamic interactions, especially in track sections with a high degree of geometrical complexity such as switches and crossings. Nevertheless, the amount of time and parameters required by MBS to carry out the preprocessing of the numerical model, including its calibration and validation, hinders its portability across the whole railway network and, hence, the use of MBS models as part of condition monitoring systems. The strength of the proposed low-complexity behavioral model is the ability to be accurate despite its simple structure. This is possible thanks to the blending of a model structure rooted into the dynamical behavior of the infrastructure with measured data through the adopted subspace identification method.

The identification of the 4-th order model representing the vertical track dynamics opens opportunities for the development of a condition monitoring system to supervise the occurrence of degradation processes affecting the ballast layer and the railpads. Long-term monitoring of the model natural frequencies and damping ratios through e.g. recursive estima-

tion of the model parameters could provide valuable insight on how the ballast layer deteriorates over time.

The obtained model is based on data from receptance test, which are seldom performed by infrastructure managers due to their cost in terms of time and money. Hence, to achieve true portability of the proposed model, a natural extension of this work is to use only measured accelerations due to train passages to identify the vertical track dynamics.

6. CONCLUSION

The paper contributes to the identification of a low-complexity behavioral model of the vertical track dynamics in correspondence of the switch panel of a railway turnout. The behavioral model was obtained by utilizing measured track accelerations collected during a receptance test in conjunction with the Eigensystem Realization Algorithm.

Analysis of the coherence function between the impact force and the measured acceleration addressed that the collected data are reliably informative about the dominant dynamics of the turnout up to 1 kHz. Therefore the bandwidth of the identified model has been limited to this value. A 4-th order model with two resonance frequencies has been consistently identified. The estimated resonance frequencies $\omega_{n,1} = 167.59$ Hz and $\omega_{n,2} = 549.96$ Hz are attributed to the ballast layer and the railpad. These values are in line with the state-of-the-art know-how for such type of structures.

The model was successfully validated on measured accelerations collected during normal train passages; this demonstrated the robustness and predictive capability of the low-complexity behavioral model.

ACKNOWLEDGMENT

The financial support under grant number 4109-00003B provided by Innovation Fund Denmark for the INTELLISWITCH project is gratefully acknowledged.

REFERENCES

Alves Costa, P., Calçada, R., & Silva Cardoso, A. (2012). Track-ground vibrations induced by railway traffic: In-situ measurements and validation of a 2.5 d fem-bem model. *Soil Dynamics and Earthquake Engineering*, *32*(1), 111-128.

Arlaud, E., Costa D'Aguiar, S., & Balmes, E. (2016). Receptance of railway tracks at low frequency: Numerical and experimental approaches. *Transportation Geotechnics*, *9*, 1-16.

Asplund, M., Larsson, D., Rantatalo, M., Nissen, A., & Kumar, U. (2013). Inspection of railway turnouts using camera. In *Proceedings of the 10th World Congress on Railway Research.* Australia.

Berggren, E. (2009). *Railway track stiffness - dynamic measurements and evaluation for efficient maintenance* (PhD Thesis). Royal Institute of Technology.

Berggren, E., Nissen, A., & Paulsson, B. (2014). Track deflection and stiffness measurements from a track recording car. *Proceedings of the Institution of Mechanical Engineers, Part F: Journal of Rail and Rapid Transit*, *228*(6), 570-580.

Brough, M., Stirling, A., Ghataora, G., & Madelin, K. (2003). Evaluation of railway trackbed and formation: a case study. *NDT & E International*, *36*(3), 145-156.

Caicedo, J., Dyke, S., & Johnson, E. (2004). Natural excitation technique and eigensystem realization algorithm for phase i of the iasc-asce benchmark problem: Simulated data. *Journal of Engineering Mechanics*, *130*(1), 49-60.

Choi, J. (2014). Qualitative analysis for dynamic behavior of railway ballasted track.

Clinton, A. (2014). *Annual Safety Performance Report 2013/14* (Tech. Rep.). Railway Safety and Standards Board.

Dahlberg, T. (2006). *Handbook of railway vehicle dynamics* (S. Iwnicki, Ed.). CRC Press.

De Man, A. (2002). *Dynatrack: A survey of dynamic railway track properties and their quality* (PhD Thesis). TU Delft.

EIM-EFRTC-CER Working Group. (2012). *Market strategies for track maintenance & renewal* (Tech. Rep. No. 2353 7473-11). CER - Community of European Railway and Infrastructure Companies.

Ewins, D. (2000). *Modal testing: Theory, Practice and Application* (2nd ed.). Research Studies Press Ltd.

Hassankiadeh, S. (2011). *Failure analysis of railway switches and crossings for the purpose of preventive maintenance* (MSc Thesis). Royal Institute of Technology.

Hosseingholian, M., Froumentin, M., & Levacher, D. (2009). Continuous method to measure track stiffness a new tool for inspection of rail infrastructure. *World Applied Sciences Journal*, *6*(5), 579-589.

Juang, J., & Pappa, R. (1985). An eigensystem realization algorithm for modal parameter identification and model reduction. *Journal of Guidance, Control, and Dynamics*, *8*(5), 620-627.

Juul Andersen, K. (2012). *Årsrapport 2012* (Tech. Rep. No. 13-00144). banedanmark.

Kaewunruen, S., & Remennikov, A. (2007). Field trials for dynamic characteristics of railway track and its components using impact excitation technique. *NDT & E International*, *40*(7), 510-519.

Kind, T. (2011). GPR antenna array for the inspection of railway ballast. In *Proceedings of the national seminar & exhibition on non-destructive evaluation.*

Labarile, A., Stella, E., Ancona, N., & Distante, A. (2004). Ballast 3D reconstruction by a matching pursuit based stereo matcher. In *Proceedings of the 2004 IEEE Intelligent Vehicles Symposium* (p. 653-657).

Lam, H., Alabi, S., & Yang, J. (2017). Identification of rail-sleeper-ballast system through time-domain Markov chain Monte Carlo-based Bayesian approach. *Engineering Structures*, *140*, 421-436.

Lam, H., Hu, Q., & Wong, M. (2014). The Bayesian methodology for the detection of railway ballast damage under a concrete sleeper. *Engineering Structures*, *81*, 289-301.

Lam, H., Wong, M., & Yang, Y. (2012). A feasibility study on railway ballast damage detection utilizing measured

vibration of in situ concrete sleeper. *Engineering Structures*, *45*, 284-298.

Majji, M., Juang, J., & Junkins, J. (2010). Time-Varying Eigensystem Realization Algorithm. *Journal of Guidance, Control, and Dynamics*, *33*(1), 13-28.

Manolakis, D., Ingle, V., & Kogon, S. (2005). *Statistical and adaptive signal processing: spectral estimation, signal modeling, adaptive filtering, and array processing* (Vol. 46). Artech House Norwood.

Oostermeijer, K., & Kok, A. (2000). Dynamic behaviour of railway superstructures. *HERON, 45 (1), 2000*.

Oregui, M., Li, Z., & Dollevoet, R. (2015). Identification of characteristic frequencies of damaged railway tracks using field hammer test measurements. *Mechanical Systems and Signal Processing*, *54-55*, 224-242.

Pappa, R., & Juang, J. (1984). Galileo spacecraft modal identification using an eigensystem realization algorithm. In *Proceedings of the 25th structures, structural dynamics and materials conference.*

Smekal, A., Berggren, E., & Silvast, M. (2006). Monitoring and substructure condition assessment of existing railway lines for upgrading to higher axle loads and speeds. In *Proceedings of the 7th World Congress on Railway Research.* Canada.

Steer Davies Gleave. (2015). *Study on the cost and contribution of the rail sector* (Tech. Rep. No. MOVE/B2/2014-761). European Commission Directorate General for Mobility and Transport.

Verbraken, H., Degrande, G., Lombaert, G., Stallaert, B., & Cuellar, V. (2013). *Benchmark tests for soil properties, including recommendations for standards and guidelines* (FP7 RIVAS Project Deliverable No. SCP0-GA-2010-265754). International Union of Railways.

Yella, S., Dougherty, M., & Gupta, N. (2009). Condition monitoring of wooden railway sleepers. *Transportation Research Part C: Emerging Technologies*, *17*(1), 38-55.

BIOGRAPHIES

Pegah Barkhordari was born in Tehran, Iran, on September 8th 1990. She has received her B.Sc. and M.Sc. degrees in Electrical Engineering from K.N. Toosi University of Technology in 2012, and Iran University of Science and Technology (IUST) in 2015, respectively. Currently she is a Ph.D. student in the Department of Electrical Engineering at the Technical University of Denmark. In her PhD project she works on data-driven condition monitoring of switches and crossing. Her research interests are fault diagnosis and prognosis, model identification, condition monitoring, and data mining.

Roberto Galeazzi was born in Ancona, Italy, on August 14th 1979. He received his M.Sc. degree in Electronic Engineering from the Technical University of Marche, Ancona, Italy, in 2005 and the Ph.D. degree in Automation and Control from the Technical University of Denmark, Lyngby, Denmark, in 2010. He is an associate professor with the Department of Electrical Engineering at the Technical University of Denmark. His research interests include fault diagnosis and prognosis, fault-tolerant and reconfigurable control, nonlinear and adaptive control, state estimation. His focus areas are safety critical systems, autonomous vehicles and wind turbines. He is the co-author of 7 ISI journal papers, 21 peer-reviewed conference papers and 2 book chapters. Further he is the co-editor of one IFAC conference proceedings. He is member of IEEE and IFAC; he seats on the IEEE Technical Committee on Aerospace Control and on the IFAC Technical Committee on Marine Systems.

Alejandro de Miguel Tejada was born in the city of Cáceres, Extremadura, Spain on June 6th 1983. He received the Ph.D. degree from the Technical University of Madrid, Spain in 2015. He currently works as a postdoc researcher at the Technical University of Denmark in the Mechanical Engineering Department (Section of Solid Mechanics). He works in the field of numerical modeling of train/track interaction, experimental measurements of track components and dynamics of structures. He is the author of 3 conference papers.

Ilmar Ferreira Santos was born in Ribeirão Preto, Sao Paulo, Brazil on April 12th 1964. He received the Dr.-Ing. Degree from the Technical University of Munich, Germany, in 1993; the livre-docente degree from State University of Campinas, Sao Paulo, Brazil in 1997 and the dr. techn. degree from the Technical University of Denmark, in 2010. He is full professor at Technical University of Denmark, Department of Mechanical Engineering. He works in the field of multiphysics design, optimization, monitoring and control of electro-mechanical machine elements. His research interests focus upon machinery dynamics, tribology, control and mechatronics. He is the author of 95 journal papers, 132 conference papers with referee, 3 books, 9 book chapters. He is member of the following professional societies: ASME American Society of Mechanical Engineering; VDI Verein Deutscher Ingenieure; ABCM Brazilian Society of Mechanical Engineering; DCAMM Danish Center of Applied Mathematics and Mechanics; STLE Society of Tribologists and Lubrication Engineers.